A FLEXIBLE ORIGAMI OPTO-ELECTRO ARRAY FOR IN VIVO OPTOGENETIC NEUROSTIMULATION AND NEUROPHYSIOLOGY RECORDING

Yan Gong^{1,4}, Xiang Liu^{2,4}, Yifan Liu^{1,4}, Zhen Qiu^{3,4}, Arthur Weber⁵, and Wen Li^{1,4}

Department of Electrical and Computer Engineering, Michigan State University, East Lansing, MI, USA

²Neuroscience Program, Department of Physiology, Michigan State University, East Lansing, MI 48824, USA

³Department of Biomedical Engineering, Michigan State University, East Lansing, Michigan, USA ⁴Institute for Quantitative Health Science and Engineering, Michigan State University, East Lansing, Michigan, USA and

⁵ Department of Physiology, Michigan State University, East Lansing, MI, USA

ABSTRACT

This paper reports a thin-film, three-dimensional (3D) opto-electro array with four individually addressable microscale light-emitting diodes (µ-LEDs) capable of surface illumination of the cortex and nine penetrating electrodes for simultaneous recording of light-evoked neural activities. Inspired by the origami concept, a carefully designed "bridge + trench" structure facilitates the conversion of the array from two-dimensional (2D) to 3D while avoiding mechanical damage to thin film metal. Before device transformation, the shape and dimensions of the 2D array can be customized, making it versatile for a variety of applications. The array is packaged using polyimide (PI) and polydimethylsiloxane (PDMS) to device's mechanical flexibility ensure the biocompatibility. The efficacy of the device is characterized both in vitro and in vivo.

KEYWORDS

Foldable probe, 2D to 3D conversion, opto-electro array, "bridge + trench" structure.

INTRODUCTION

Recordings of electrophysiological activity from neurons represent well-established essential sources of information for quantitative investigations of neural processes and for the development of biomedical systems and brain-computer interfaces [1, 2]. To better capture electrophysiological signals to understand the movement patterns and principles of muscles and nerves, many implantable devices have been evolving over the years through advances in microelectromechanical systems (MEMS) technology and deepening knowledge of neural activity and brain [3-5]. Despite device advancements, major challenges still exist, including those related to conventional 2D fabrication methods and practical requirements of 3D sharp [6-9], as well as issues such as acquisition accuracy of neural signals and collateral damage of implantable device [10-13], among many other challenges. Under the constraints of the above-mentioned challenges, device design is like a game of balance. In terms of the mechanical properties of implantable probes, flexible implantable probes are difficult to implant and require some means of strength reinforcement [14]. However, increased stiffness may induce foreign object response and thus affect behavior and nerve signal quality in various ways [15, 16]. Choosing a less aggressive strategy such as a surface-mounted electrode design may improve biocompatibility but may also have decreased signal acquisition accuracy due to distance from the nerve [17]. The above-mentioned challenges will affect the acquisition of electrophysiological signals to varying degrees.

To overcome these challenges, we proposed an origami array that integrates multiple functions for optogenetic stimulation and electrophysiological recording (Fig. 1A). With a novel "bridge+trench" structure, the origami array can be readily bent from a 2D to a 3D array without altering probe sensitivity. In addition, this unique

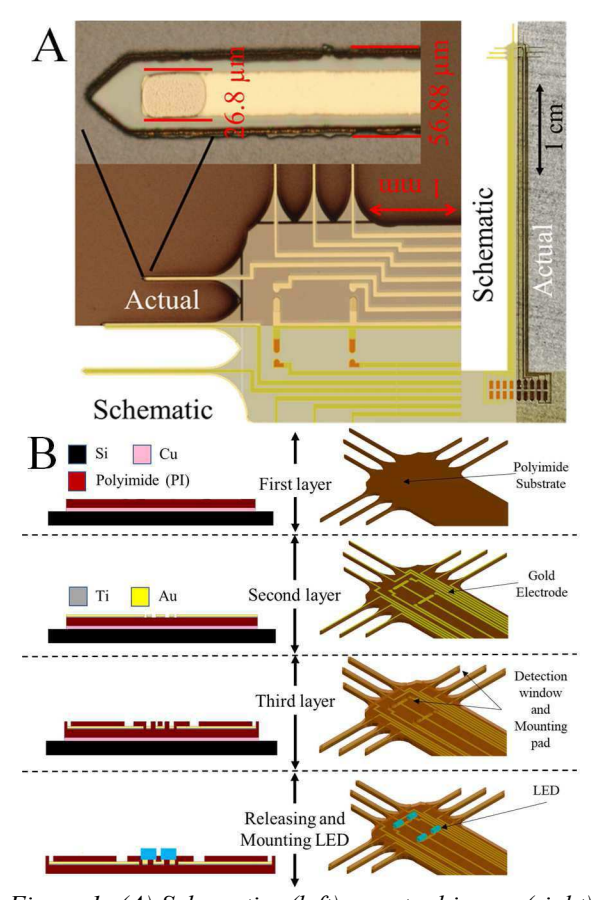


Figure 1: (A) Schematics (left) vs actual image (right) of the origami array. (B) Cross-sectional and 3D illustrations of device fabrication process flow.

design minimizes mechanical damage to metal traces at the bends while allowing the geometry and dimension of each probe in the array to be customized as needed.

METHODS

Fig. 1B depicts the core fabrication process flow of the opto-electro array. Specifically, a 5 µm thick layer of copper was electroplated on a 4-inch-diameter silicon wafer as a sacrificial layer. Adhesion promoter (VM652, HD Microsystems L.L.C. NJ, USA) was spun on the wafer in advance to improve the adhesion of polyimide. PI (PI2611, HD Microsystems L.L.C. NJ, USA) was spun on the adhesion promoter at a spinning speed of 4000 rpm, resulting in the thickness of PI at $\sim 6 \mu m$. Then the wafer will be baked on a hotplate for soft-baking at 90 °C for 3 mins and 150°C for 3 mins to thicken PI, followed by hardbaking at an elevated temperature of 350 °C for ~30 mins to cure the PI. The cured PI will completely dissociate the carrier solvent, fully imidine the film and complete polymer orientation, thereby optimizing its dielectric and mechanical properties. After PI was cured, 200 nm copper layer was thermally evaporated on the PI layer as the hard mask, photoresist (PR, S1813, Shipley, Marlborough, MA) was spun onto the copper to form the probe shape through photolithography, followed by wet etching of copper. The basic probe shape was defined using reactive ion etching at a power of 200 W and gas pressure of 0.15 Torr for 20 mins. After that, titanium (20 nm) and gold (200 nm) was thermal evaporated as the electrode material, and the designed electrodes and traces were patterned using chemical wet etching with a photolithographically defined PR mask. Another PI layer was coated in the same way to encapsulate the probe and selectively patterned to define the recording sites and mounting pads. After the device was released from the wafer, four blue μ -LEDs were assembled on the designated mounting pads. To do that, a small amount of tack flux (CHIPQUIK® Tack Flux SMD291ST2CC6, Life solution Inc, Ancaster, ON) and low-temp solder paste (CHIPQUIK® LOWTEMP LEAD-FREE SN42/BI58 Solder Paste SMDLTLFP, Life solution Inc, Ancaster, ON) were applied on the pads. After the solder was melted with a hot air gun, the $\mu\text{-LEDs}$ (Cree® TR2227TM LEDs, Cree, Inc. Durham, NC) were gently placed on the corresponding pads and fine-tuned using a needle. The electrode shanks were folded along the trench structure by a needle station. The trench design plays a critical role in inducing folding and limiting the folding area. After the folding was completed, dip coating and curing of epoxy (Chemical Engineering Canada Corporation, Port Coquitlam, BC, Canada) yielded a semicircle dielectric layer of epoxy over the μ-LED for encapsulation fix the bottom of the folding array at the same time.

For device characterization, optical measurements of the μ -LEDs light output were performed with a digital power meter (PM100D, power meter and S120VC, photodiode sensor, Thorlabs, NJ, USA). The electrochemical impedance of the microelectrodes was measured with an electrochemical analyzer (Model 600E Series, CH Instruments, Inc., Austin, TX, USA). The functionality of the device for neural stimulation and

recording was evaluated in the primary visual cortex (V1) of a rat that was genetically modified with AAV-hSynhChR2(H134R)-mCherry based on our established protocols [18]. Using sterile surgical procedures, the virus solution $(10\times10^{11} \sim 10\times10^{12} \text{ vector genome (vg)/mL, UNC})$ Vector Core, Chapel Hill, NC) was injected in the V1 of a Sprague-Dawley rat (male, 350-400 g). After injection, the animal was housed in the animal facility for 2-4 weeks to allow cells to express channelrhodopsin-2 (ChR2). For acute experiments, the transfected rat was re-anesthetized and placed back into the stereotaxis. The device was surgically implanted over the V1 and the stimulation and recording tests were conducted. Post-surgery immunohistology processing followed a standard c-Fos protocol. The anesthetized rat's brain was stimulated for 45 mins, followed by a 90 mins survival period. Later, the rat was perfused with chilled phosphate-buffered saline (PBS) and 4% paraformaldehyde, post-fix brain overnight at 4°C in the same solution. Brain sections were cut to 40 µm thick, chilled in 0.1 M PBS, and placed in culture dishes. Sections were washed three times for 10 mins in PBS. Then sections were soaked in PBS mixing 1% NGS and 0.3% Triton X-100 for 2hrs at room temperature (23°C). One m of rabbit mAb antibodies were placed in 1.5 mL Eppendorf tubes. Tubes were clipped onto a rotating mixer and stored at 40 °C for 24 hrs incubation. Sections were poured into culture dishes in the dark with 20 antibodies (ThermoFisher A27034 goat anti-rabbit IgG superclonal Alexa Fluor 488 conjugate) for 2 hrs at room temperature. Finally, sections were washed in 0.1 M PBS, mounted and cover slipped with anti-fade media and stored in a cool dark place. All procedures were approved by the Institutional Animal Care and Use Committee (IACUC) at Michigan State University.

RESULTS AND DISCUSSION

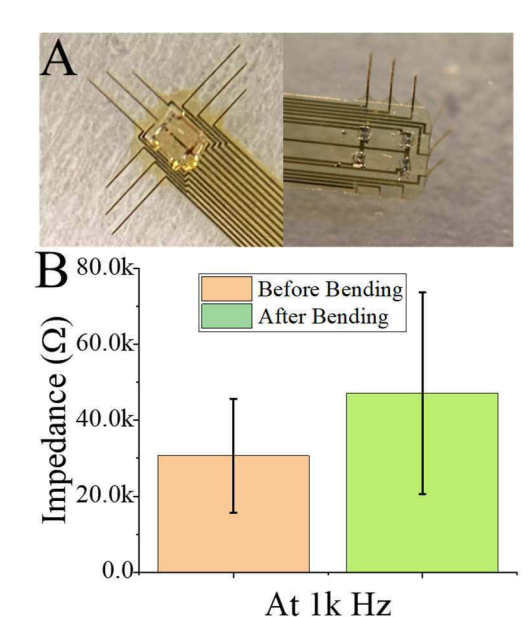


Figure 2: (A) The images of the array before (left) and after bending (right). (B) The impedance changes before and after bending.

Folding is a necessary process to achieve the transformation from a 2D array to a 3D form, and it is a key function of origami probes. However, the change in impedance during the folding process raises concerns. Fig. 2A illustrates the state after folding, showing that each probe was perpendicular to the LED array at 90 degrees. Fig. 2b shows that such folding, without any special design, can cause severe damage to the thin metal layer inside the probes, leading to a significant increase in the 1kHz electrochemical impedance. Based on previous research [19], metal damage due to mechanical stress during bending is one of the potential causes of this impedance change. Based on this hypothesis, the solution revolves around how to reduce stress-indued metal damage. Since folding is inevitable, the first idea is to reduce the stress on the metal trace during folding, by isolating the metal part from other parts of the probe, making it as stress-free as possible. The second idea is to widen the metal traces at the bending points in order to compensate for some of the metal breakage. Combining these two approaches leads to a uniquely designed "bridge-type" structure. Moreover, a "trench" structure allows bending to occur at relatively fixed positions, facilitating structural design and preventing other parts of the probe from folding. Finite element simulation in COMSOL Multiphysics, Solid Mechanics Model (COMSOL, Inc., Burlington, MA, USA) (Fig. 3A) confirms that the bridge structure can distribute the mechanical stress more uniformly across the bending junction, thereby improving the device's stability. From the comparison of the left and right images in Fig. 3A, where the left side shows the "bridge + trench" structure, it's evident that this design disperses stress over a larger area compared to the right side, where stress is more concentrated along a line. Consequently, the maximum stress in the "bridge + trench" structure is relatively reduced. Fig. 3B displays, from top to bottom, the "wide

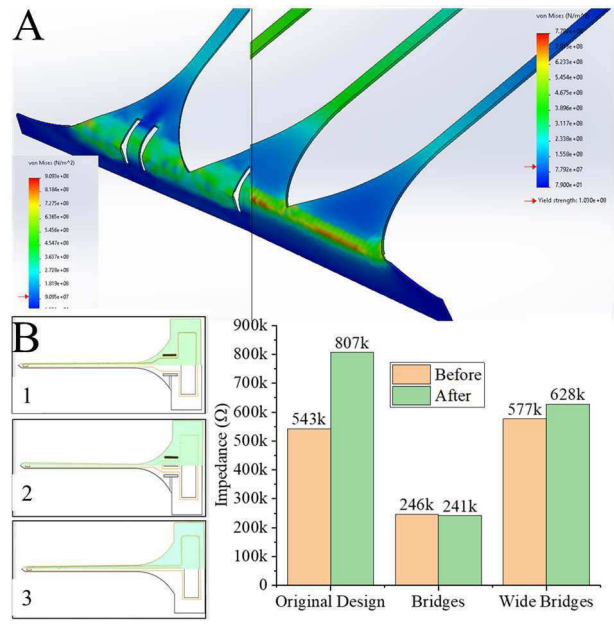


Figure 3: (A) Finite element analysis of stress distribution between the bridge design (left) and the original design (right), (B) 1-Wide bridge, 2-Narrow bridge, and 3-Original designs, and their impedance changes after bending.

bridge," "double bridge," and the original designs. Fig. 3C demonstrates that the bridge-type structures, in both designs, effectively improved the stability in electrochemical impedance after folding as compared to the original design that still experienced an increase in impedance after folding.

Fig. 4A shows device validation in acute animal experiments. The penetrating electrodes were able to record spontaneous single-unit responses at 0.6 mm depth without LED stimulation. With LED stimulation, increasing neural activity with higher amplitude spikes was observed, indicating that blue light stimulation can effectively activate ChR2 and induce neural activity (Fig.

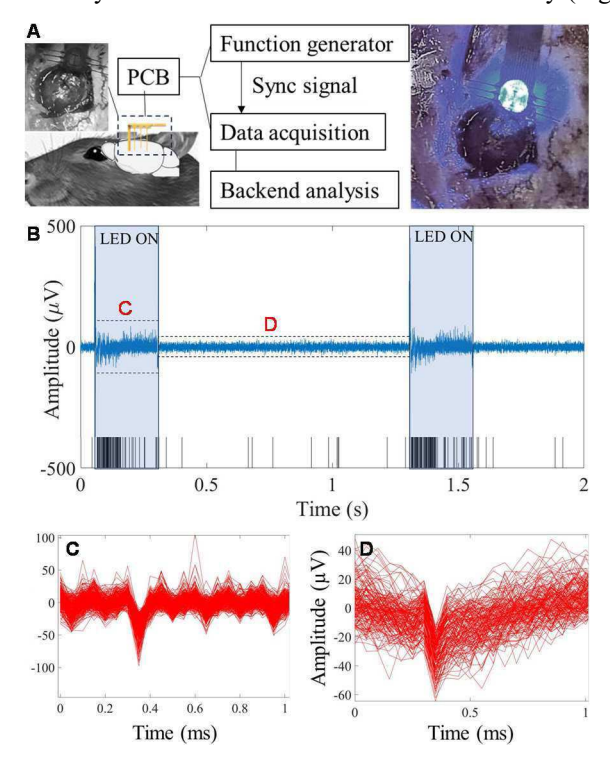


Figure 4: (A) In vivo experiment setup. (B) Neural activity during two cycles of LED stimulation (200 ms ON and 800 ms OFF), with each black bar representing a neural spike captured. Optical input power at 20 mW/mm². (C) Sorted neural spikes recording in Imin during and after the LED stimulation. (D) Sorted neural spikes in 1 min before the LED stimulation.

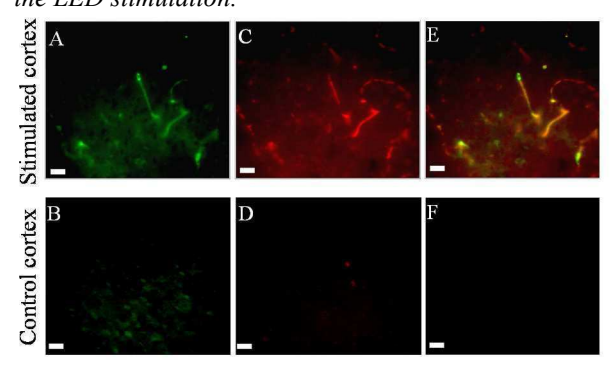


Figure 5: Immunohistology analysis showing c-Fos (A, B) and mCherry (C, D) expressions in the stimulated and control visual cortex. (E, F) The combined images. Scale bar = $25\mu m$.

4B). The efficacy of optogenetic neurostimulation was further validated using immunohistology analysis post-stimulation, showing a higher population of neurons expressing c-Fos biomarker in the stimulated cortex (Fig. 5A) in comparison with the control cortex (Fig. 5B).

CONCLUSION

The conclusion drawn from the presented results emphasizes the successful integration of innovative design and functional application in the development of origami probes for neurostimulation/neurorecording. The necessity of folding in transforming a 2D array into a 3D form is effectively managed by the "bridge + trench" structure, which not only accommodates the inherent process of folding but also significantly mitigates the stress-induced damage to the metal layers within the probes. This is evidenced by the COMSOL simulations and the comparative analysis of the "bridge + trench" structure with traditional designs (Fig. 3). The reduced maximum stress and the maintained impedance post-folding highlight the efficacy of this novel design approach.

Furthermore, the practical application of these probes in the V1 of a genetically modified rat showcases their functionality in a real-world setting. The ability of the penetrating electrodes to record spontaneous single-unit responses, as well as the increased neural activity under LED stimulation, as observed in Fig. 4B, demonstrates the probes' effectiveness in optogenetic neurostimulation and neurophysiology recording. The increased expression of the c-Fos biomarker in stimulated neurons, compared to the control cortex (Fig. 5), further validates the efficacy of the LED light stimulation in inducing neural activity.

In conclusion, the integration of innovative structural design in origami probes with their effective application illustrates an advancement in the field of optoelectronic stimulation and recording array. The "bridge + trench" structure effectively addresses the challenges posed by folding-induced stress and impedance changes, ensuring the structural integrity and functional stability of the probes.

ACKNOWLEDGEMENTS

This project is supported by the National Science Foundation under award numbers ECCS-2024270.

REFERENCES

- [1] Y. Zhang *et al.*, "Battery-free, fully implantable optofluidic cuff system for wireless optogenetic and pharmacological neuromodulation of peripheral nerves," *Science Advances*, vol. 5, no. 7, p. eaaw5296, 2019.
- [2] W. Ouyang *et al.*, "A wireless and battery-less implant for multimodal closed-loop neuromodulation in small animals," *Nature Biomedical Engineering*, pp. 1-18, 2023.
- [3] Y. U. Cho, S. L. Lim, J.-H. Hong, and K. J. Yu, "Transparent neural implantable devices: A comprehensive review of challenges and progress," *npj Flexible Electronics*, vol. 6, no. 1, p. 53, 2022.
- [4] B. Lu *et al.*, "Neuronal Electrophysiological Activities Detection of Defense Behaviors Using

- an Implantable Microelectrode Array in the Dorsal Periaqueductal Gray," *Biosensors*, vol. 12, no. 4, p. 193, 2022.
- [5] I. Mastoris *et al.*, "Emerging implantable-device technology for patients at the intersection of electrophysiology and heart failure interdisciplinary care," *Journal of cardiac failure*, vol. 28, no. 6, pp. 991-1015, 2022.
- [6] G. D. Goh, J. M. Lee, G. L. Goh, X. Huang, S. Lee, and W. Y. Yeong, "Machine learning for bioelectronics on wearable and implantable devices: challenges and potential," *Tissue Engineering Part A*, vol. 29, no. 1-2, pp. 20-46, 2023.
- [7] T. van Manen, S. Janbaz, M. Ganjian, and A. A. Zadpoor, "Kirigami-enabled self-folding origami," *Materials Today*, vol. 32, pp. 59-67, 2020.
- [8] C. Yang, H. Zhang, Y. Liu, Z. Yu, X. Wei, and Y. Hu, "Kirigami-Inspired Deformable 3D Structures Conformable to Curved Biological Surface," *Advanced Science*, vol. 5, no. 12, p. 1801070, 2018.
- [9] Z. Yan *et al.*, "Controlled mechanical buckling for origami-inspired construction of 3D microstructures in advanced materials," *Advanced functional materials*, vol. 26, no. 16, pp. 2629-2639, 2016.
- [10] K. Na *et al.*, "Novel diamond shuttle to deliver flexible neural probe with reduced tissue compression," *Microsystems & Nanoengineering*, vol. 6, no. 1, p. 37, 2020.
- [11] C. Henle *et al.*, "First long term in vivo study on subdurally implanted micro-ECoG electrodes, manufactured with a novel laser technology," *Biomedical microdevices*, vol. 13, no. 1, pp. 59-68, 2011.
- [12] M. Shaeri, A. Afzal, and M. Shoaran,
 "Challenges and opportunities of edge ai for
 next-generation implantable BMIs," in 2022
 IEEE 4th International Conference on Artificial
 Intelligence Circuits and Systems (AICAS), 2022:
 IEEE, pp. 190-193.
- [13] N. S. Witham *et al.*, "Flexural bending to approximate cortical forces exerted by electrocorticography (ECoG) arrays," *Journal of neural engineering*, vol. 19, no. 4, p. 046041, 2022.
- [14] Y. Shi, R. Liu, L. He, H. Feng, Y. Li, and Z. Li, "Recent development of implantable and flexible nerve electrodes," *Smart Materials in Medicine*, vol. 1, pp. 131-147, 2020.
- [15] J. M. Anderson, A. Rodriguez, and D. T. Chang, "Foreign body reaction to biomaterials," in *Seminars in immunology*, 2008, vol. 20, no. 2: Elsevier, pp. 86-100.
- [16] Y. Onuki, U. Bhardwaj, F. Papadimitrakopoulos, and D. J. Burgess, "A review of the biocompatibility of implantable devices: current challenges to overcome foreign body response," *Journal of diabetes science and technology,* vol. 2, no. 6, pp. 1003-1015, 2008.

- [17] M. E. E. Alahi, Y. Liu, Z. Xu, H. Wang, T. Wu, and S. C. Mukhopadhyay, "Recent advancement of electrocorticography (ECoG) electrodes for chronic neural recording/stimulation," *Materials Today Communications*, vol. 29, p. 102853, 2021.
- [18] K. Y. Kwon, B. Sirowatka, A. Weber, and W. Li, "Opto-μECoG array: A hybrid neural interface with transparent μECoG electrode array and integrated LEDs for optogenetics," *IEEE transactions on biomedical circuits and systems*, vol. 7, no. 5, pp. 593-600, 2013.
- [19] E. Korzeniewska, G. De Mey, R. Pawlak, and Z. Stempień, "Analysis of resistance to bending of metal electroconductive layers deposited on textile composite substrates in PVD process," *Scientific Reports*, vol. 10, no. 1, pp. 1-11, 2020.

CONTACT

*Yan Gong, tel: +1-517-402-6197; gongyan@msu.edu